BMC Cancer

RESEARCH

Open Access

Comprehensive analysis identifies YKT6 as a potential prognostic and diagnostic biomarker in lung adenocarcinoma

Liming Zhang[1,2], Shaoqiang Wang[3] and Lina Wang[1*]

Abstract

Background Lung cancer is the most common cause of cancer-related death worldwide. The most prevalent histological subtype of lung cancer is lung adenocarcinoma (LUAD), with incidence rising each year. Treating LUAD remains a significant issue due to a lack of early diagnosis and poor therapy outcomes. YKT6 is a member of the SNARE protein family, whose clinical value and biological function in LUAD has yet to be established.

Methods TCGA, HPA and UALCAN were used to analyze YKT6 mRNA and protein levels, the correlation between YKT6 expression and clinicopathological features and prognosis. YKT6 mRNA and protein expression were verified by qRT-PCR, immunohistochemistry (IHC) and tissue microarrays (TMA). Additionally, lung cancer cell lines were chosen for YKT6 silencing to explore the effects on cell proliferation and migration. The cBioPortal was used to select YKT6-related genes. Protein-protein interaction (PPI) network was created based on STRING database and hub genes were screened, with their expression levels and prognosis values in LUAD analyzed accordingly. YKT6-related genes were enriched by gene ontology (GO) and Kyoto encyclopedia of genes and genomes (KEGG) analyses.

Results In LUAD, YKT6 was distinctly highly expressed with relation to clinical features of staging, smoking, lymph node metastasis, and TP53 mutation. Elevated YKT6 expression was linked to adverse prognosis, serving as an independent unfavorable prognostic factor. Moreover, YKT6 presented high diagnostic value in LUAD patients (AUC = 0.856). Experimental validation indicated that freshly collected LUAD tissues showed significantly high mRNA expression of YKT6. IHC and TMA verified increased YKT6 protein level in LUAD. Knockdown of YKT6 inhibited cell proliferation and promoted apoptosis, with mitigated capability of migration and invasion. The top ten hub genes screened by PPI network were highly expressed in LUAD, and significantly associated with poor prognosis. GO and KEGG analyses showed that YKT6-related genes were mainly involved in cell cycle.

Conclusion Elevated YKT6 expression is related to poor prognosis of LUAD patients. YKT6 can serve as a novel biomarker for LUAD diagnosis and prognosis. Cell proliferation, migration and invasion was impaired with increased apoptosis upon YKT6 silencing in lung cancer cells. In summary, this study comprehensively uncovered that YKT6 could be identified as a potential prognostic and diagnostic biomarker in LUAD.

Keywords Lung adenocarcinoma (LUAD), YKT6, Prognosis, Biomarker, Bioinformatics analysis

*Correspondence:
Lina Wang
wanglina_china@163.com

Full list of author information is available at the end of the article

Introduction

Based on the latest Global Cancer Statistics for 2022, lung cancer has been identified as the most prevalent form of cancer, with nearly 2.5 million new cases diagnosed, representing a significant global health burden. Furthermore, it stands as the foremost cause of cancer-related mortality, claiming approximately 1.8 million lives and constituting 18.7% of all cancer-related fatalities [1]. According to the different tissue types, lung cancer can be classified into small cell lung cancer (SCLC) and non-small cell lung cancer (NSCLC), the latter accounting for about 85% of total lung cancer. Lung adenocarcinoma (LUAD) is the most common type of NSCLC, with 40% of all lung cancer [2]. With the popularity of computed tomography (CT) in early screening of lung cancer, the prognosis of patients with LUAD has been significantly improved, alongside the overall understanding of the early diagnosis and effective prevention strategies for early LUAD [3, 4]. However, the onset of LUAD is hidden, and the majority of patients are in an advanced stage at the time of diagnosis. Thus, patients failed to undergo surgery, less sensitive to radiotherapy or chemotherapy, resulting in a 5-year survival rate of less than 15% [5, 6]. In recent years, targeted therapy has achieved favorable consequences in lung cancer patients; however, its power to combat tumor progress is limited due to the current clinical treatment [7]. Therefore, it is very important to discover novel potential biomarkers for early diagnosis and prognosis evaluation of LUAD.

YKT6 belongs to the soluble N-ethylmaleimide sensitivity factor attachment protein receptor (SNARE) family, with molecular weight 23 kDa [8, 9]. YKT6 has no transmembrane domain, but with an N-terminal login domain and a C-terminal SNARE domain, which interacts to form a folded or closed conformation [10]. Studies have reported that YKT6 is related to vesicle transport, involved in the process of cell membrane fusion, as well as exosome formation and release, which is highly conserved in eukaryotes [11]. Yang et al. has found that YKT6 is highly expressed in oral squamous cell carcinoma (OSCC), related to the poor prognosis and can promote the invasion and metastasis of OSCC cells [12]. Previous research has shown that YKT6 is highly expressed in hepatocellular carcinoma (HCC), and its expression is significantly correlated with tumor size, microvascular invasion, and alpha-fetoprotein (AFP) level [13]. In addition, YKT6 was up-regulated in breast cancer with docetaxel-resistant P53 mutation, and knockdown of YKT6 could enhance DXT-induced apoptosis in breast cancer cells [14]. Based on the above evidence, it is speculated that YKT6 might play an important role in the occurrence, development, and drug resistance in many tumor types. However, the potential biological role of YKT6 in LUAD has not yet been reported until now.

Thus, in our present study, the molecular characteristic analysis was performed to evaluate the potential function of YKT6 in the diagnosis and prognosis of LUAD. Moreover, the fundamental in vitro experiments were conducted to verify its biological function in lung cancer cells. Finally, gene-gene and protein-protein interaction (PPI) network and functional enrichment analyses were carried out to determine the function of YKT6 in LUAD. Therefore, this study indicates that YKT6 can function as a novel prognostic and diagnostic biomarker in LUAD.

Materials and methods

Expression of YKT6 mRNA in pan-cancer

The Cancer Genome Atlas (TCGA) [15] (https://portal.gdc.cancer.gov/) is jointly established by the National Cancer Institute (NCI) and the National Human Genome Research Institute (NHGRI). A total of 36 cancer types are studied, including mutation, copy number variation, mRNA expression, miRNA expression, methylation, and other data. We downloaded and extracted the RNA-seq data of pan-cancer and LUAD from TCGA database, processed the data, excluded missing and repeated samples, statistically analyzed and visualized the results using the ggplot2 package, and analyzed the mRNA expression of YKT6 in pan-cancer and LUAD.

Expression of YKT6 protein in LUAD

The Human Protein Atlas (HPA) database [16] (https://www.proteinatlas.org/) uses transcriptome and proteomics methods to study protein expression in various human tissues and organs at mRNA and protein levels. HPA database was used to compare YKT6 protein levels in LUAD and para-cancerous tissues.

RNA extraction and qRT-PCR

LUAD and para-cancerous tissues were freshly collected. None of the patients had received preoperative treatment. Informed consent was obtained from all participants prior to the study. The Ethics Committee of the Affiliated Hospital of Jining Medical University evaluated and approved this work (Approval number 2021-11-C009). The total RNA was extracted with TRIzol reagent, and RNA concentration was determined. The cDNA was obtained by reverse transcription by DNA synthesis kit HiScript III RT SuperMix for qPCR (+gDNA wiper) for qRT-PCR. GAPDH was loaded as an internal reference, and the relative expression was calculated by the $2^{-\Delta\Delta Ct}$ method. The synthetic sequences of relevant primers are listed in Supplementary Table 1.

Immunohistochemistry (IHC) and tissue microarray (TMA)

The LUAD and para-cancerous tissues were embedded in paraffin. Continuous 4 μm slices were dewaxing, plugging, incubating with the primary antibody (anti-YKT6,

ab236583) overnight at 4 °C; then adding the secondary antibody, incubating at room temperature for 2 h, and analyzing the signal with an optical microscope. The human LUAD tissue microarray (ZL-Lug961) was provided by Shanghai Zhuoli Biotechnology Co., Ltd. (Shanghai, China), and the protein levels of YKT6 was assessed by the automated VisioMorph system (Visiopamm ®, Hoersholm, Denmark).

Correlation between YKT6 expression and clinicopathological features

Download RNA-seq data and clinical information of LUAD project from TCGA database, exclude normal tissue and samples without clinical information, then analyze the data with stats (4.2.1).

Survival analysis of YKT6 in LUAD

Kaplan-Meier plotter was used to explore the relation between YKT6 expression and overall survival (OS), recurrence free survival (RFS) of LUAD patients [17, 18].

Diagnostic value of YKT6 in LUAD

The receiver operating characteristic (ROC) curve was drawn by R package pROC to analyze the RNA-seq data in FPKM format from LUAD project in TCGA database. The ggplot2 package was used for visualization.

Immune infiltration analysis

Download LUAD data from TCGA, extract the expression data of YKT6, and use the ssGSEA algorithm in the GSVA package to analyze the immune cell infiltration [19]. Using multiple algorithms, such as MCP-counter, XCELL, and TIMER (https://cistrome.shinyapps.io/timer/) to evaluate the correlation between YKT6 expression and immune cell infiltration in LUAD [20].

Cell culture and siRNA transfection

Human lung cancer cell lines (A549 and Calu-1) were kindly provided by Wuhan Pricella Biotechnology Co.,Ltd, which were cultured in a 37 °C CO_2 incubator with RPMI-1640 medium plus 10% fetal bovine serum (FBS). Cells were incubated in a 6-well plate, and siRNA mixed with Lipofectamine 3000 were added into the medium for transfection. The YKT6 siRNA sequences are as follows:

Si-1 (YKT6–Homo-684): Sense: GCUGGGAACACAG UCUAAATT.

Anti-Sense: UUUAGACUGUGUUCCCAGCTT.

Si-2 (YKT6-Homo-257): Sense: CCAGCGUUCAGGA AUUCAUTT.

Anti-Sense: AUGAAUUCCUGAACGCUGGTT.

Cell proliferation assay by cell counting kit-8 (CCK-8)

2×10^3 cells were inoculated into a 96-well plate, and 10 μL CCK-8 solution was added to each well at 0 h, 24 h, 48 h, and 72 h, respectively, and incubated at 37 °C for 2 h. The absorbance at 450 nm was analyzed with standard microplate readers (BioTek, Winsky, Vermont, USA).

Scratch wound healing assay

5×10^5 cells per well were seeded in six-well plates. After covering the monolayer, the cells were scratched with the 10 μL tips and washed with PBS. The medium without FBS was added to continue the culture. The pictures were taken under a microscope at 0 h and 24 h, and analyzed by ImageJ software.

Transwell assay

3×10^5 cells were inoculated and cultured in a six-well plate. 600 μL medium was added to the lower chamber, and 100 μL cells in serum-free RPMI-1640 medium were added to the upper chamber. After being cultured at 37°C for 24, 36, and 48 h, the chamber was inverted on absorbent paper to drain the medium, followed by rinsing with PBS. Then the chamber was fixed with 4% paraformaldehyde for 20 min, followed by staining with crystal violet (0.1%) for 15 min. Non-metastatic cells in the chamber were then removed by cotton swabs. Finally, images were captured under a microscope, and processed by ImageJ software.

Detection of apoptosis after YKT6 silencing by flow cytometry

Annexin V-FITC Apoptosis Detection Kit (C1062L, Beyotime Biotechnology, China) was used for the detection of cell apoptosis. The cultured cells were harvested and collected via centrifugation, washed thrice with PBS, and resuspended in 100 μL staining buffer. Subsequently, 5 μL Annexin V-FITC and 5 μL propidium iodide were added to the cells, which were then maintained on ice for 15 min in the dark. Apoptosis rate was detected using a DxFLEX flow cytometer (BECKMAN).

Construction of gene-gene and PPI network with hub genes screening

Gene-gene interaction network was constructed via GeneMANIA [21] (http://genemania.org/). The cBioPortal database [22](https://www.cbioportal.org/) integrates data of somatic mutation, DNA copy number change, mRNA and miRNA expression, protein and phosphoprotein abundance, which can perform mutation correlation analysis and visualization. First, we log into the database to select the top 100 positively correlated genes of YKT6 based on Spearman's correlation. Then, STRING database (https://cn.string-db.org) [23] and Cytoscape

(Version 3.9.0) [24] were utilized to build the PPI network and screen the top ten hub genes according to the degree scores.

GO and KEGG enrichment analysis

The DAVID website [25, 26] (https://david.ncifcrf.gov/) is a health information database with systematic biological function annotation information for a large number of genes and proteins. The selected top 100 YKT6-related genes were analyzed by GO and KEGG using the DAVID database to explore the possible biological process, cellular component, molecular function, and pathways involved. The Chiplot (https://www.chiplot.online/#BioPlot) website was used to visualize the enrichment analyses.

GSEA

Download the RNA-seq data and clinical information of LUAD project from TCGA database. Extract the expression data of the corresponding molecules, divide them into two groups according to the expression of the molecules, and use the DESeq2 package to analyze the single gene difference of the data. The data set comes from the MSigDB Collections database (https://www.gsea-msigdb.org/gsea/msigdb/collections.jsp). Then, we use the org.hs.eg.db package for ID conversion of the differential genes and the clusterprofiler package for GSEA.

Statistical method

All the statistical data were analyzed by SPSS (Version 22.0) software. The data are expressed as mean ± standard deviation (SD). The differences between subgroups were compared using a 2-tail paired *t*-test. $^{*}P<0.05$ was considered to be statistically significant.

Results

The expression of YKT6 mRNA in pan-cancer and LUAD

Firstly, we explored the expression of YKT6 mRNA in pan-cancer. The results showed that YKT6 was highly expressed in bladder urothelial carcinoma (BLCA), breast invasive carcinoma (BRCA), cholangiocarcinoma (CHOL), colon adenocarcinoma (COAD), esophageal carcinoma (ESCA), head and neck squamous cell carcinoma (HNSC), kidney chromophobe (KICH), kidney renal clear cell carcinoma (KIRC), kidney renal papillary cell carcinoma (KIRP), liver hepatocellular carcinoma (LIHC), lung adenocarcinoma (LUAD), lung squamous cell carcinoma (LUSC), prostate adenocarcinoma (PRAD), stomach adenocarcinoma (STAD), uterine corpus endometrial carcinoma (UCEC), but low in thyroid carcinoma (THCA) (Fig. 1A). In addition, the unpaired samples from TCGA and Genotype-tissue expression (GTEx) showed that YKT6 mRNA expression was significantly elevated in adrenocortical carcinoma (ACC), BLCA, BRCA, cervical squamous cell carcinoma and endocervical adenocarcinoma (CESC), CHOL, COAD, lymphoid neoplasm diffuse large B-cell lymphoma (DLBC), ESCA, glioblastoma multiforme (GBM), HNSC, KICH, KIRP, brain lower grade glioma (LGG), LIHC, LUAD, LUSC, ovarian serous cystadenocarcinoma (OV), pancreatic adenocarcinoma (PAAD), PRAD, rectum adenocarcinoma (READ), skin cutaneous melanoma (SKCM), STAD, testicular germ cell tumors (TGCT), thymoma (THYM), UCEC, and uterine carcinosarcoma (UCS) (data not shown). Thus, YKT6 expressed highly in almost all the tumor types except acute myeloid leukemia (LAML) and THCA.

Based on the unpaired and paired samples in TCGA and GTEx, YKT6 mRNA showed significantly elevated expression in LUAD (Fig. 1B-C). HPA revealed that YKT6 protein was weakly stained or not detected in normal lung tissues, but moderately stained in LUAD tissues (Fig. 1D-E). Therefore, YKT6 mRNA/protein expression in LUAD tissues is higher than that in normal lung tissues.

Validation of the elevated expression of YKT6 in LUAD tissues

Tissue samples from patients with LUAD were collected and performed qRT-PCR. Compared to para-cancerous tissues, YKT6 mRNA was expressed highly in LUAD tissue samples (Fig. 2A). Immunohistochemical (IHC) staining and tissue microarray analysis (TMA) showed that YKT6 protein was significantly elevated in LUAD tissues (Fig. 2B-F).

Moreover, YKT6 mRNA expression was validated by GSE31547, GSE40791, and GSE43458. Consistently, in all these LUAD samples, YKT6 displayed obviously increased expression compared to normal groups (Fig. 2G-I). Hence, the elevated expression of YKT6 was verified at both mRNA and protein levels by these external LUAD tissue samples.

Prognostic and diagnostic value of YKT6 in LUAD

The association between YKT6 expression and LUAD prognosis was examined using the transcriptome and clinical data from TCGA. There was a substantial correlation between high YKT6 expression and poor OS and RFS (Fig. 3A-B). The univariate and multivariate Cox regression revealed that YKT6 expression and pathologic M stage emerged as independent risk factors for the prognosis of LUAD patients (Fig. 3C-D and Supplementary Table 2). Afterwards, a nomogram was created to predict the survival of LUAD patients at 1-, 3-, and 5-year (Fig. 3E). Thus, YKT6 is an independent risk factor, and elevated YKT6 expression indicates adverse outcome in LUAD.

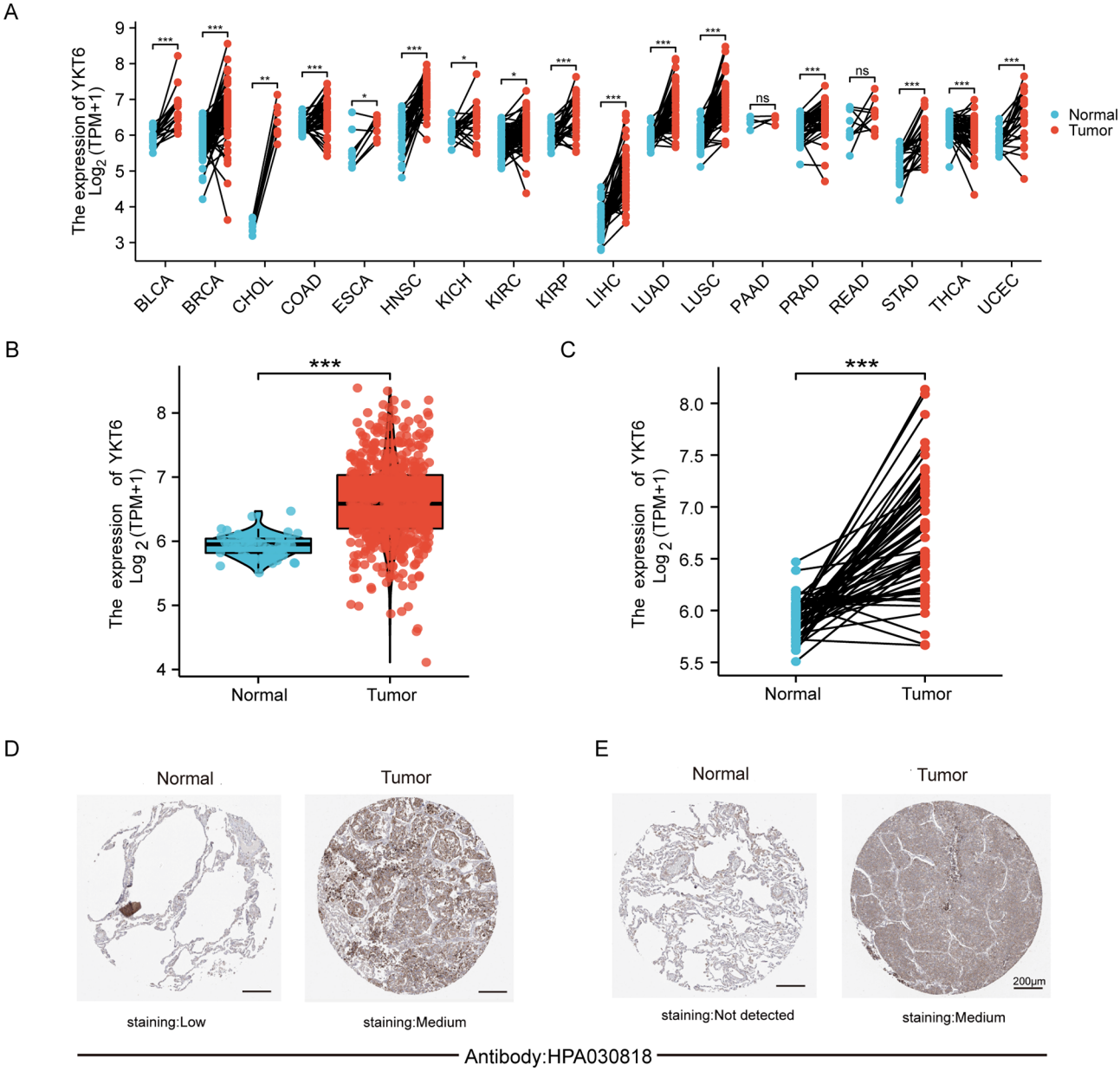

Fig. 1 The mRNA and protein expression of YKT6 in LUAD based on TCGA. (**A**) Expression of YKT6 mRNA in paired tissues of pan-cancer in TCGA. (**B**)-(**C**) YKT6 mRNA expression in unpaired and paired LUAD tissues. (**D**)-(**E**) YKT6 protein levels in LUAD of HPA

In addition, the receiver operating characteristic (ROC) curve was utilized to determine the diagnostic ability of YKT6 in distinguishing tumor and normal samples. Notably, the area under the curve (AUC) value was up to 0.856, demonstrating high diagnostic value in LUAD patients (Fig. 3F).

Correlation between YKT6 expression and clinicopathological features

The correlation between the expression of YKT6 and LUAD clinicopathological features was analyzed in TCGA. YKT6 mRNA demonstrated a statistically significant correlation with the pathological N stage, pathological stage, primary therapy outcome, age, number pack years smoked, OS, and disease-specific survival (DSS) (Table 1).

Immune infiltration analysis of YKT6 in LUAD

MCP-counter were used to explore the immune cell infiltration of CRGs in LUAD. Based on YKT6 mRNA expression, TCGA samples were split into two groups. MCP-counter findings revealed that T cells, B cells, endothelial cells and myeloid dendritic cells are the substantially distinct immune cell types invaded between

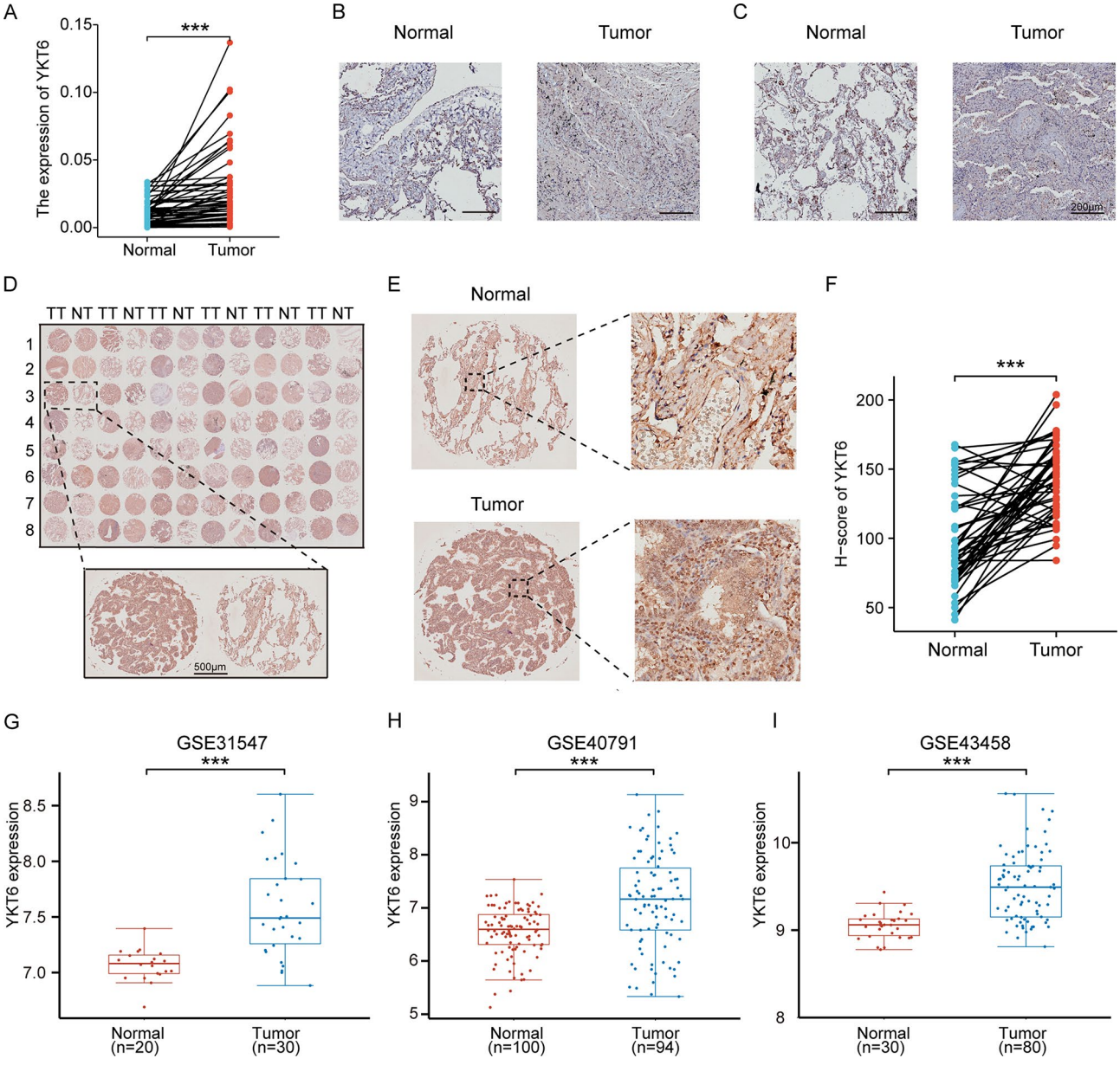

Fig. 2 Validation of YKT6 expression by LUAD tissues and GEO. (**A**) Detection of YKT6 mRNA expression in LUAD by qRT-PCR. (**B**)-(**C**) The representative immunohistochemistry staining of YKT6 in LUAD. (**D**) Tissue microarray analysis of YKT6 expression in LUAD and normal tissues. (**E**) The representative IHC staining of YKT6 in LUAD and para-cancerous tissues. (**F**) YKT6 staining was analyzed by H-score in LUAD and para-cancerous tissues. (**G**)-(**I**) YKT6 mRNA expression in GSE31547, GSE40791, and GSE43458

YKT6 high and low expression samples (Fig. 4A). We used the ssGSEA algorithm and Spearman analysis to search the association between YKT6 and 24 kinds of immune cell infiltration. The results showed that Th2 cells, Tgd, NK CD56dim cells, NK cells, and Treg cells were positively correlated with the expression of YKT6, whereas mast cells, B cells, DC, $CD8^+$ T cells, T cells, and central memory T cells (Tcm) were negatively correlated with YKT6 expression (Fig. 4B). Additionally, TIMER analysis also demonstrated a connection between YKT6 expression and $CD4^+$/$CD8^+$ T cells and B cells (Fig. 4C). According to the findings of the XCELL analysis, YKT6 expression was associated with $CD8^+$ T cells, Th2, Th1, DC, M2, B cells and common lymphoid progenitors (Fig. 4D).

Knockdown of YKT6 inhibits cell proliferation and promotes apoptosis of lung cancer cells

YKT6 mRNA expression was significantly reduced in A549 and Calu-1 cells upon silencing by siRNA transfection. Cell proliferation assay by CCK-8 showed that YKT6 knockdown inhibited A549 and Calu-1 cell

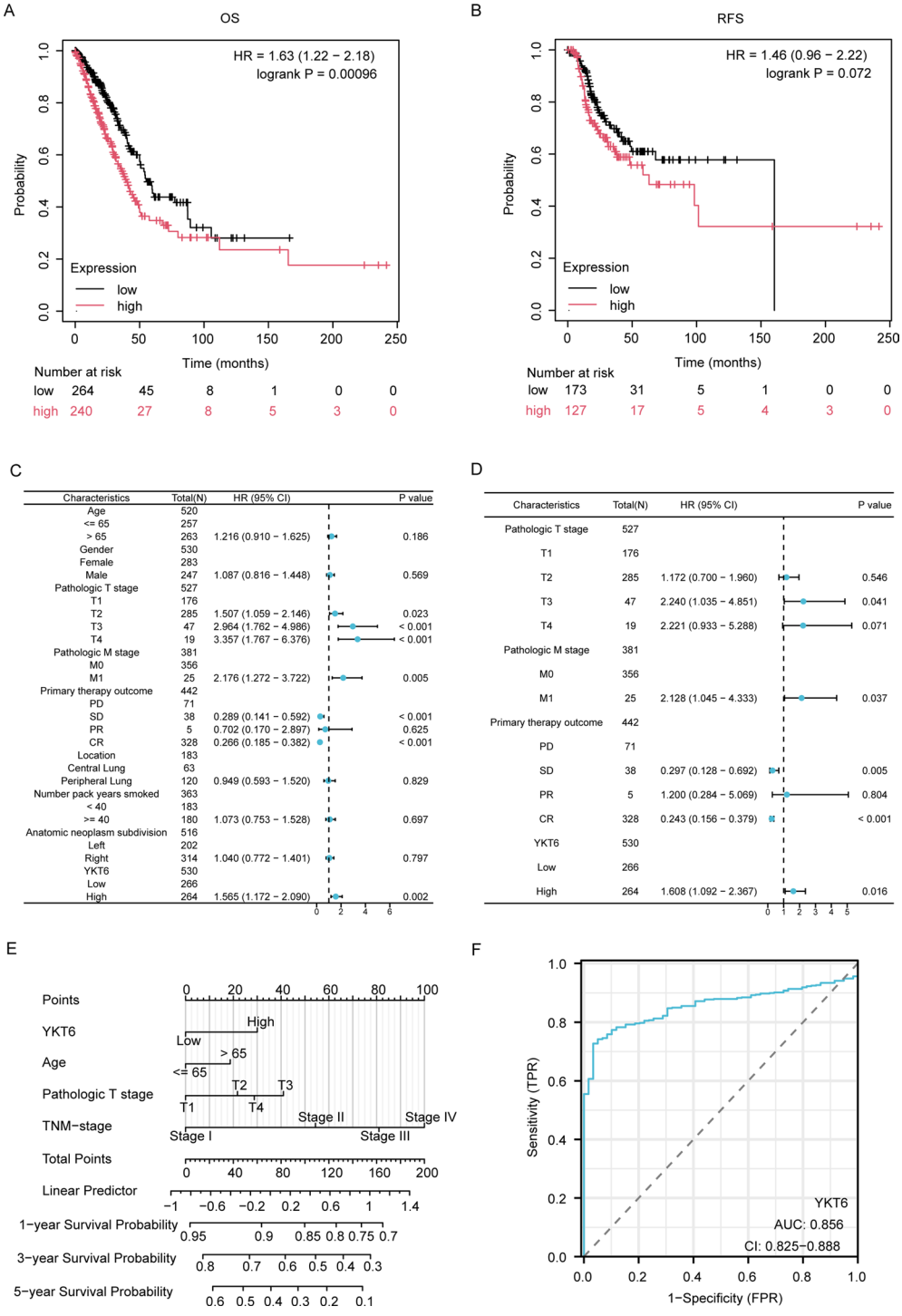

Fig. 3 Prognostic and diagnostic value of YKT6 in LUAD. (**A**)-(**B**) The relationship between YKT6 mRNA expression and OS, RFS in LUAD patients. (**C**)-(**D**) The univariate and multivariate Cox analysis of YKT6 in LUAD. (**E**) Nomogram of YKT6 in LUAD. (**F**) ROC curve of YKT6 in LUAD

proliferation (Fig. 5A-B). In addition, the flow cytometry analysis revealed obviously increased Annexin V^+ cells after YKT6 silencing in A549 and Calu-1 cells (Fig. 5C-D). Thus, YKT6 knockdown could inhibit cell proliferation and promote apoptosis of lung cancer cells.

In order to explore the underlying molecular mechanism of YKT6 in LUAD, cell proliferation-related genes were examined after YKT6 knockdown. The results demonstrated that TGF-b, Ki-67, Hes1, Cyclin-B1, Cyclin-E2 and CDK9 expression was considerably suppressed upon silencing of YKT6 in these cells (Fig. 5E-F). Based on

Table 1 Correlation between YKT6 expression and clinicopathological features

Characteristics	Low expression of YKT6	High expression of YKT6	*P* value
n	269	270	
Pathologic T stage, n (%)			0.078
T1	102 (19%)	74 (13.8%)	
T2	136 (25.4%)	156 (29.1%)	
T3	22 (4.1%)	27 (5%)	
T4	8 (1.5%)	11 (2.1%)	
Pathologic N stage, n (%)			**< 0.001**
N0	191 (36.5%)	159 (30.4%)	
N1	44 (8.4%)	53 (10.1%)	
N2	22 (4.2%)	52 (9.9%)	
N3	0 (0%)	2 (0.4%)	
Pathologic M stage, n (%)			0.754
M0	187 (47.9%)	178 (45.6%)	
M1	12 (3.1%)	13 (3.3%)	
Pathologic stage, n (%)			**0.002**
Stage I	163 (30.7%)	133 (25%)	
Stage II	60 (11.3%)	65 (12.2%)	
Stage III	26 (4.9%)	58 (10.9%)	
Stage IV	13 (2.4%)	13 (2.4%)	
Primary therapy outcome, n (%)			**0.014**
PD	25 (5.6%)	46 (10.2%)	
SD	22 (4.9%)	16 (3.6%)	
PR	1 (0.2%)	5 (1.1%)	
CR	175 (39%)	159 (35.4%)	
Gender, n (%)			0.760
Female	146 (27.1%)	143 (26.5%)	
Male	123 (22.8%)	127 (23.6%)	
Race, n (%)			0.275
Asian	2 (0.4%)	6 (1.3%)	
Black or African American	26 (5.5%)	29 (6.1%)	
White	212 (44.9%)	197 (41.7%)	
Age, n (%)			**0.007**
<= 65	114 (21.9%)	143 (27.5%)	
> 65	148 (28.5%)	115 (22.1%)	
Histological type, n (%)			0.136
Lung Adenocarcinoma- Not Otherwise Specified (NOS)	158 (30.4%)	182 (35.1%)	
Lung Papillary Adenocarcinoma	13 (2.5%)	10 (1.9%)	
Lung Adenocarcinoma Mixed Subtype	57 (11%)	52 (10%)	
Lung Bronchioloalveolar Carcinoma Nonmucinous	11 (2.1%)	8 (1.5%)	
Lung Acinar Adenocarcinoma	12 (2.3%)	6 (1.2%)	
Mucinous (Colloid) Carcinoma	8 (1.5%)	2 (0.4%)	
Residual tumor, n (%)			0.438
R0	183 (48.9%)	174 (46.5%)	
R1	8 (2.1%)	5 (1.3%)	
R2	1 (0.3%)	3 (0.8%)	
Anatomic neoplasm subdivision, n (%)			0.843
Left	105 (20%)	102 (19.5%)	
Right	158 (30.2%)	159 (30.3%)	
Location, n (%)			0.436
Central Lung	26 (13.7%)	37 (19.5%)	
Peripheral Lung	60 (31.6%)	67 (35.3%)	
Number pack years smoked, n (%)			**0.014**
< 40	106 (28.7%)	82 (22.2%)	

Table 1 (continued)

Characteristics	Low expression of YKT6	High expression of YKT6	*P* value
>= 40	79 (21.4%)	102 (27.6%)	
Smoker, n (%)			0.599
No	36 (6.9%)	41 (7.8%)	
Yes	224 (42.7%)	224 (42.7%)	
OS event, n (%)			**0.008**
Alive	188 (34.9%)	159 (29.5%)	
Dead	81 (15%)	111 (20.6%)	
DSS event, n (%)			**0.026**
No	201 (40%)	182 (36.2%)	
Yes	49 (9.7%)	71 (14.1%)	
PFI event, n (%)			0.236
No	163 (30.2%)	150 (27.8%)	
Yes	106 (19.7%)	120 (22.3%)	

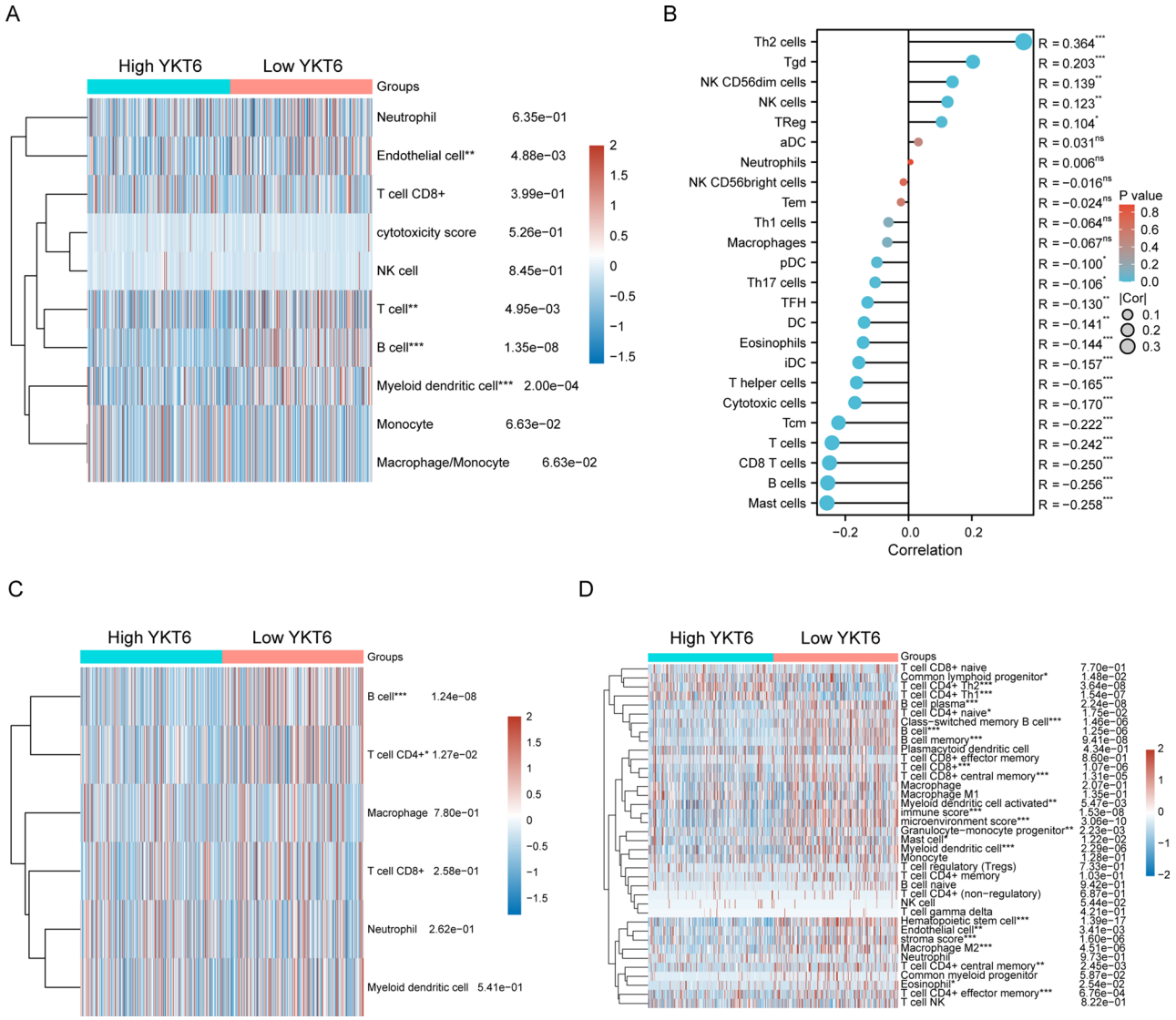

Fig. 4 The immune cell infiltration analysis of YKT6 in LUAD. (**A**) The association between YKT6 expression and immune cells infiltration in LUAD based on MCP-counter. (**B**) Lollipop diagram displaying the correlation between YKT6 expression and 24 immune cells infiltration. (**C**)-(**D**) The relation between YKT6 expression and immune infiltration in LUAD based on TIMER (**C**) and XCELL (**D**). **P* < 0.05, ***P* < 0.01, ****P* < 0.001

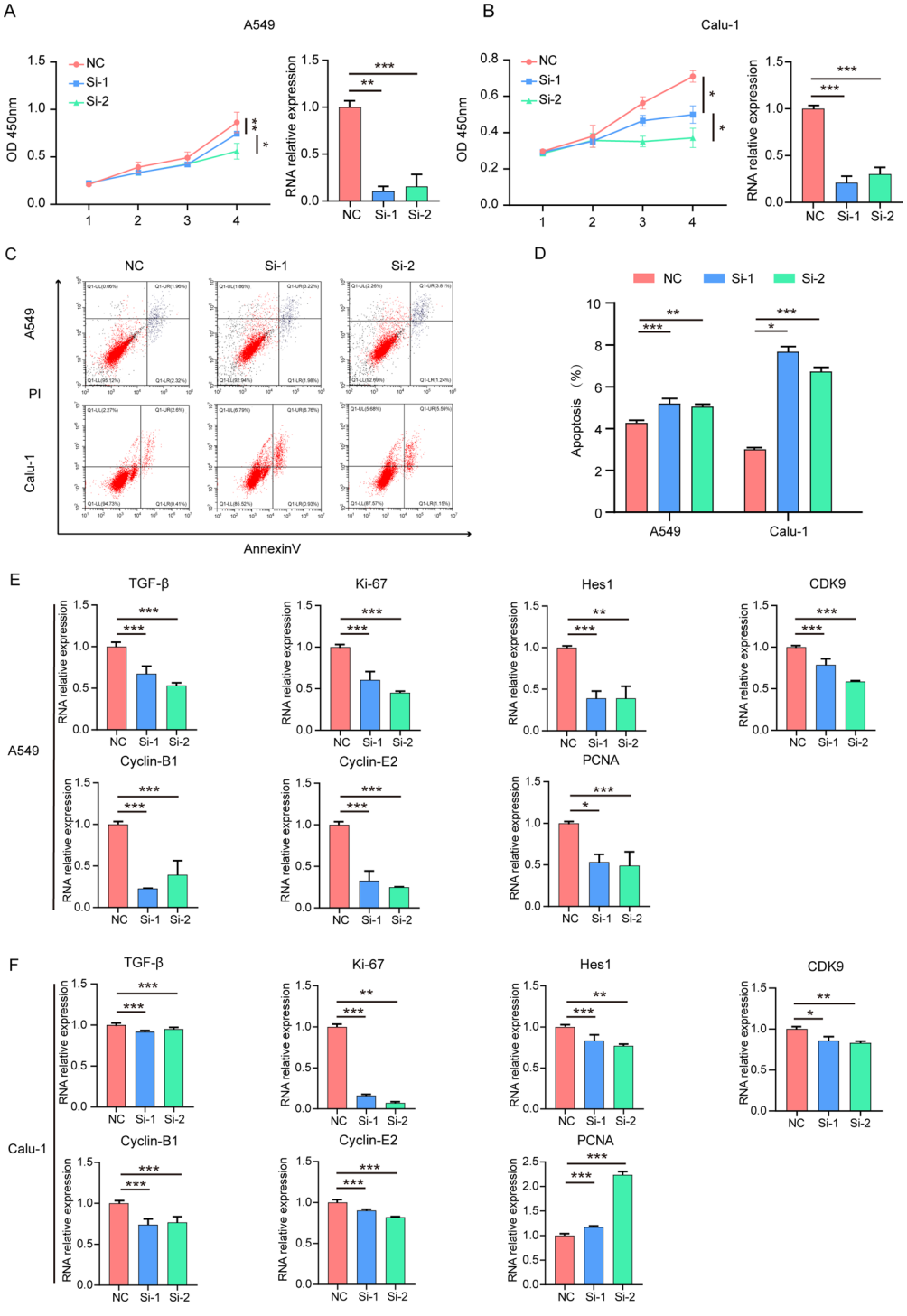

Fig. 5 Knockdown of YKT6 inhibits proliferation and facilitates apoptosis of LUAD cells. Cell proliferation was inhibited in A549 (**A**) and Calu-1(**B**) cells detected by CCK-8 assay after YKT6 silencing. (**C**)-(**D**) Increased Annexin V + apoptotic cells in A549 and Calu-1cells analyzed by flow cytometry upon YKT6 knockdown. (**E**)-(**F**) The mRNA expression of TGF-b, Ki-67, Hes1, Cyclin-B1, Cylin-E2 and CDK9 was verified after YKT6 was knocked down in A549 and Calu-1 cells by qRT-PCR

these results, it is speculated that YKT6 might play a role through cell cycle related genes in LUAD.

YKT6 silencing inhibits cell migration and invasion

The scratch wound healing experiment demonstrated that cell migration ability was decreased upon YKT6 silencing in A549 and Calu-1 cells (Fig. 6A-B). Similarly, Knockdown of YKT6 reduced cell capacity of invasion in the Transwell assay in A549 and Calu-1 cells (Fig. 6C). Hence, YKT6 knockdown could inhibit cell migration and invasion of lung cancer cells. Thus, it is speculated that YKT6 might be involved in the regulation of cell migration via EMT-related factors. Consistently, the results demonstrated that EMT-related genes including Slug, Twist1, and Snail were remarkably decreased when YKT6 was knocked down in A549 and Calu-1 cells (Fig. 7A-B). Moreover, YKT6 might play a role in LUAD through PLK1 pathway as demonstrated by GSEA (Fig. 7C and Supplementary Fig. 1). TCGA database indicated that PLK1 was highly expressed in LUAD, with a strong positive correlation (R=0.589) to YKT6 (Fig. 7D-E). Meanwhile, the in vitro cellular function analysis showed an obvious PLK1 mRNA decrease upon YKT6 silencing in lung cancer cells (Fig. 7F-G).

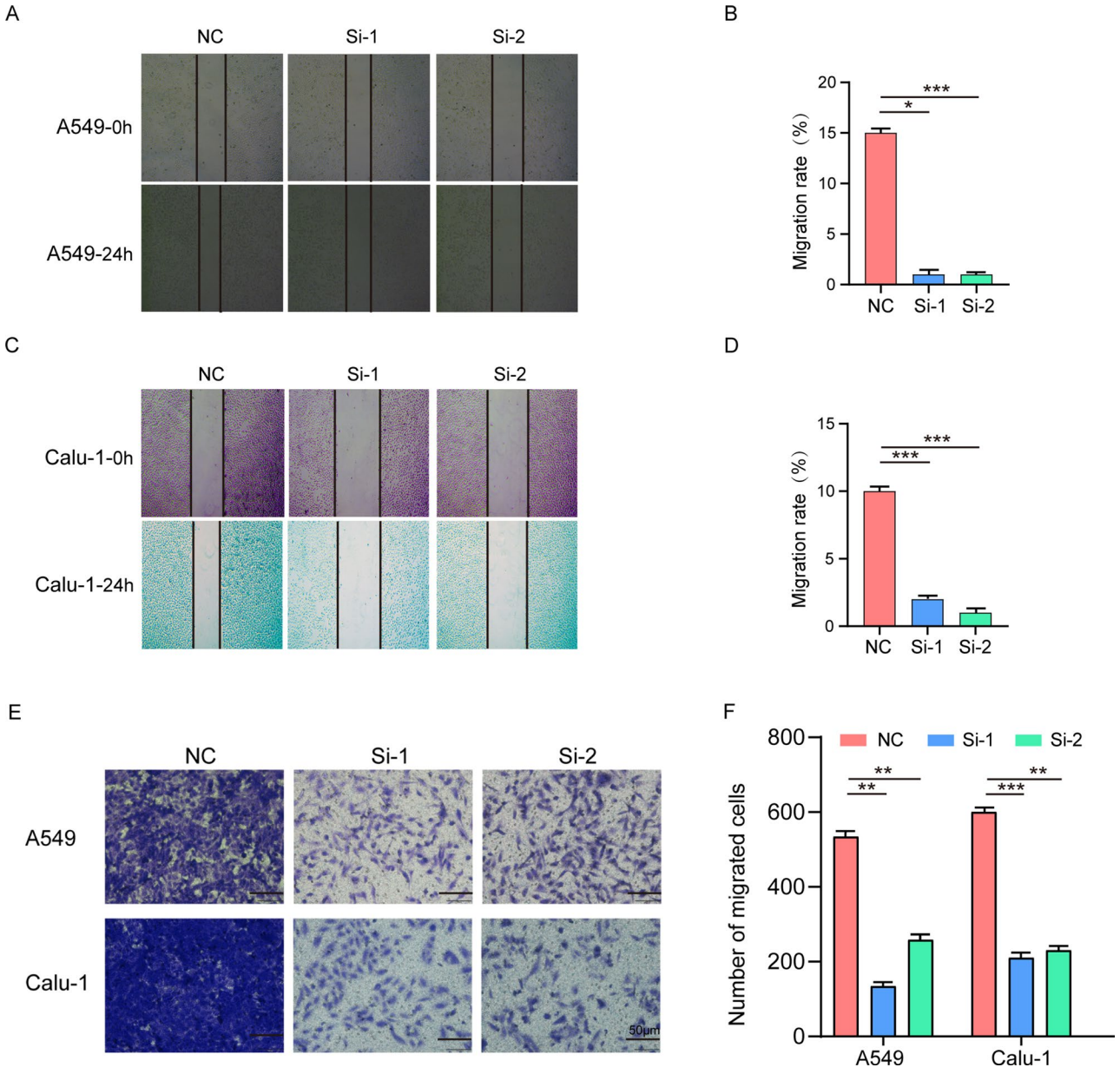

Fig. 6 YKT6 silencing attenuates migration and invasion of lung cancer cells. Scratch wound healing assay to determine the migration ability of A549 (**A**-**B**) and Calu-1(**C**-**D**) cells after YKT6 silencing. (**E**)-(**F**) The impaired invasive ability of A549 and Calu-1 cells was detected by Transwell assay

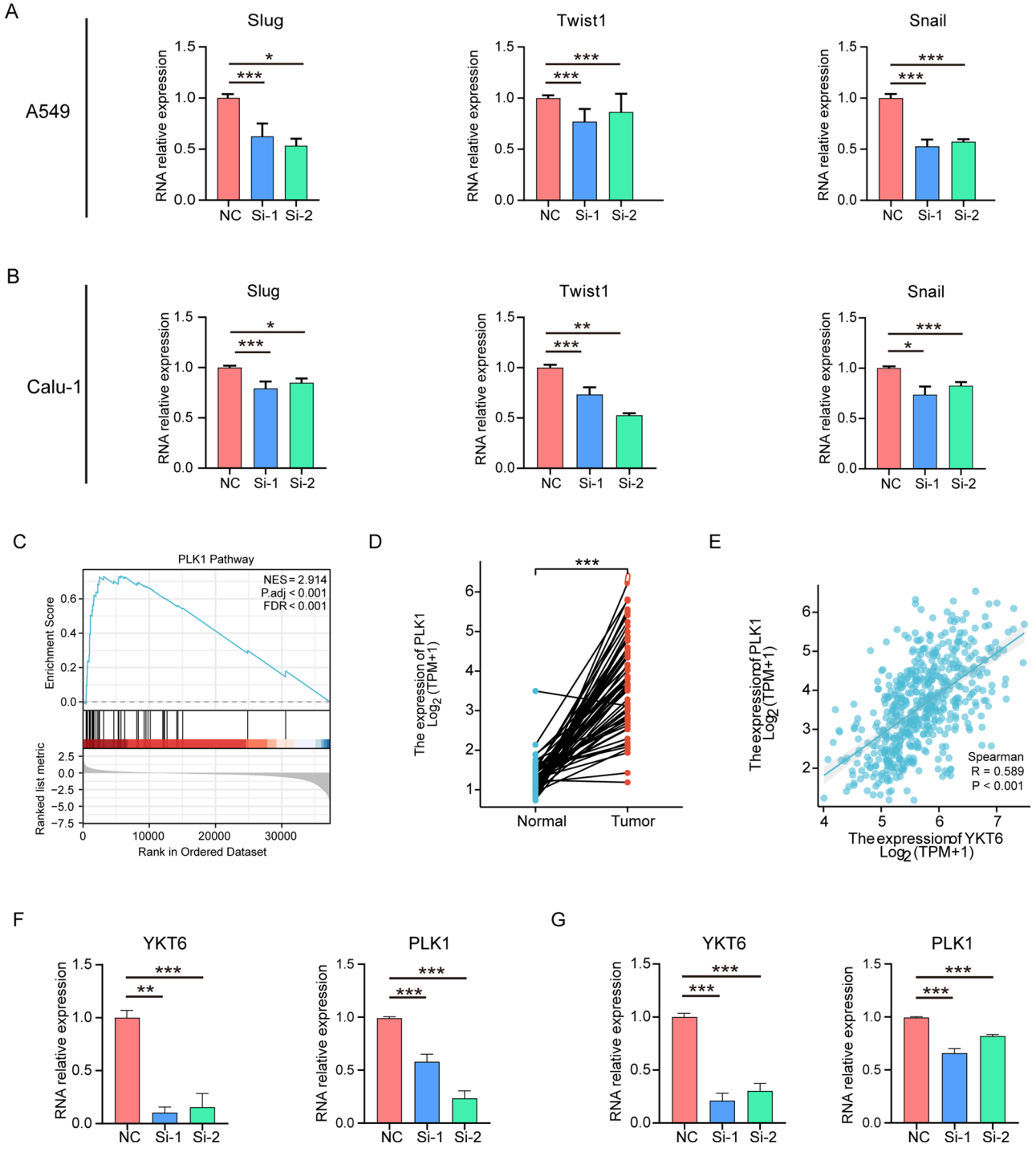

Fig. 7 Knockdown of YKT6 inhibits the expression of EMT-related genes and PLK1. The expression of Slug, Twist1, and Snail was verified upon YKT6 silencing in A549 (**A**) and Calu-1 (**B**) cells by qRT-PCR. (**C**) PLK1 pathway was screened out by GSEA of differentially expressed genes (DEGs) of YKT6 in LUAD. (**D**) Expression of PLK1 mRNA in paired LUAD tissues based on TCGA database. (**E**) The scatter plot of the correlation between YKT6 and PLK1 in LUAD of TCGA. (**F**)-(**G**) PLK1 mRNA expression was decreased upon YKT6 silencing in A549 and Calu-1 cells detected by qRT-PCR

Construction of gene-gene interaction and PPI network with hub genes screening

The YKT6-related gene-gene interaction network was created via Genemania (Fig. 8A). The cBioPortal database was used to obtain YKT6 related genes and the top 100 genes were selected based on the Spearman values (Supplementary Table 3). Subsequently, the STRING database was used to construct PPI network and the top ten hub genes were screened as follows: CDC20, PLK1, CDCA8, TPX2, KIF2C, KIF23, KIF4A, FOXM1, MCM7

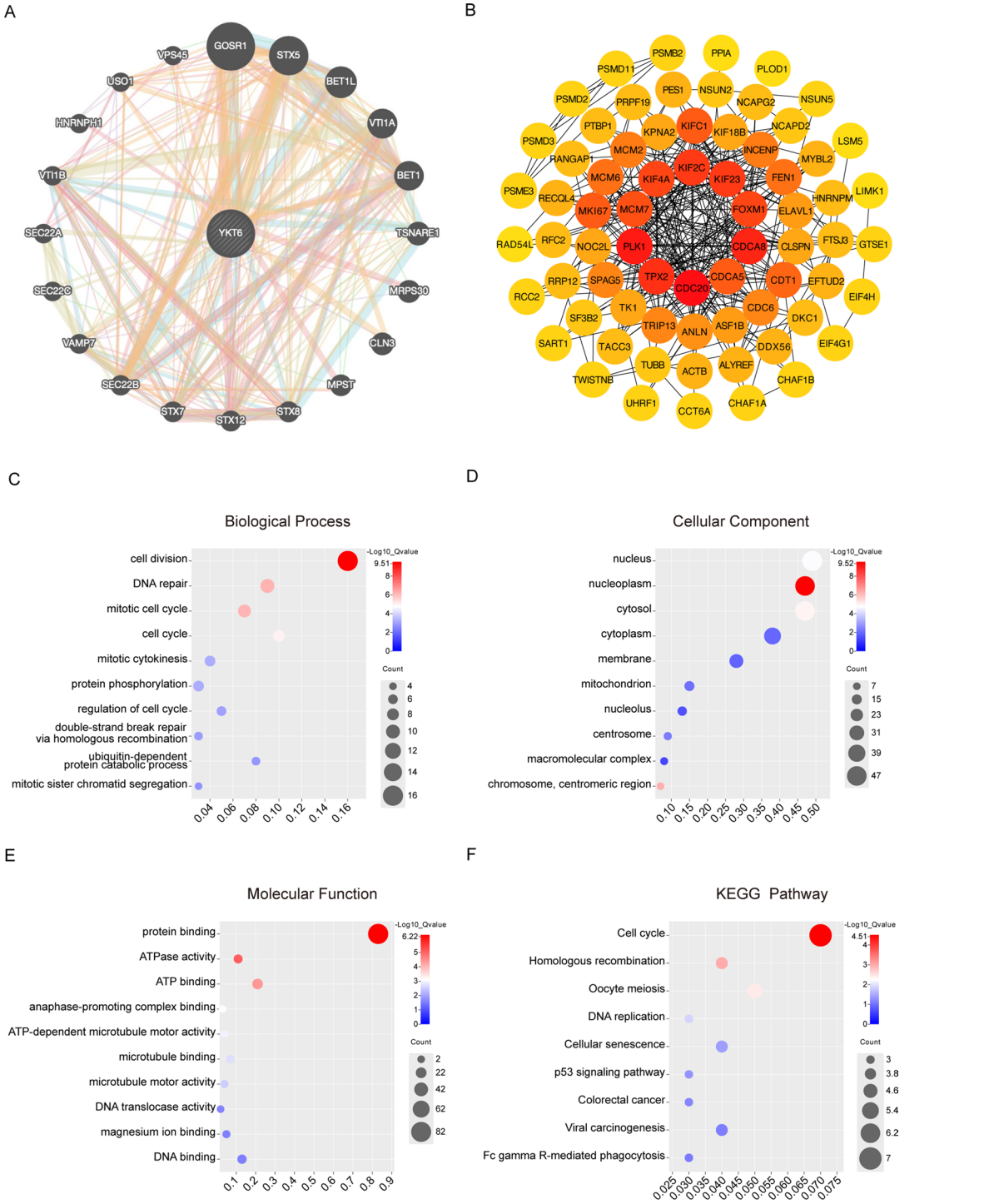

Fig. 8 Integrated analysis of gene-gene network, PPI and functional enrichment analysis of YKT6 and its related genes. (**A**) Creation of gene-gene network via Genemania. (**B**) PPI Network of YKT6 and related genes. (**C**) Biological process, (**D**) Cellular component, (**E**) Molecular function, and (**F**) KEGG pathway of YKT6 and its related genes

and CDCA5 (Fig. 8B). Additionally, TCGA data and clinical information showed that the selected ten hub genes were all highly expressed in LUAD (Supplementary Fig. 2), with relation to poor prognosis of LUAD patients (Supplementary Fig. 3).

GO and KEGG enrichment analyses of YKT6 and related genes

GO and KEGG enrichment analyses were conducted through the DAVID database to explore the potential biological functions of YKT6 and its co-expressed

genes. They were mainly involved in cell division, DNA repair, mitosis, and cell cycle (Fig. 8C), primarily located in nuclear cytoplasm, cytoplasm, cell membrane, and mitochondria (Fig. 8D). Their major molecular functions including protein binding, ATP enzyme activity, and ATP binding (Fig. 8E), with potential mechanisms through cell cycle, cell senescence, and p53 signal pathway (Fig. 8F). Based on these findings, there is reason to propose that the crucial biological role of YKT6 in LUAD might be mainly involved in cell cycle.

Discussion

Lung cancer remains one of the leading causes of cancer-related mortality globally [27]. Within this spectrum, LUAD stands as the predominant histological subtype, with its incidence on the rise annually [28]. Nonetheless, the prognosis for LUAD patients leaves much to be desired, primarily due to the challenges associated with early detection [29]. While advancements in radiotherapy, chemotherapy, surgical interventions, and targeted therapies have notably enhanced the survival rates for LUAD patients, the disease continues to pose a formidable challenge to global public health [30]. Consequently, there is an immediate imperative to identify novel diagnostic biomarkers and therapeutic targets for LUAD.

This study, leveraging a combination of clinical samples and in vitro experiments, compellingly demonstrated that YKT6 possesses the capacity to influence apoptosis, EMT, as well as the proliferation, migration, and invasion of cancer cells. These revelations propose that the targeting of YKT6 could represent a promising therapeutic strategy for lung cancer treatment. In the present research, we observed that YKT6 mRNA and protein were overexpressed in LUAD, showing significant correlations with clinical stage, lymph node metastasis, smoking history, and TP53 mutations in LUAD (Supplementary Fig. 4). Notably, YKT6 expression peaked in clinical stage III and lymph node metastasis stage IV, indicating a potentially significant role in the intermediate and advanced stages of LUAD. This suggests that YKT6 could serve as a potential indicator for LUAD staging. Furthermore, YKT6 expression was found to be elevated in TP53-mutated tissues compared to TP53-non-mutated LUAD samples, implying that YKT6 may play a crucial role in LUAD progression via the TP53 pathway. Additionally, a significant correlation between YKT6 expression and OS and RFS was observed, proposing YKT6 as a potential prognostic biomarker for LUAD. We acknowledge the necessity for an expanded collection of clinical samples and patient data to substantiate the mRNA and protein expression levels of YKT6, to explore its correlation with clinical and pathological features, and to analyze its association with patient survival times. This need represents a limitation of our current study. Moving forward, we are committed to amassing a larger cohort of high-quality, paired specimens to reinforce and validate our findings.

Among the top ten hub genes (CDC20, PLK1, CDCA8, TPX2, KIF2C, KIF23, KIF4A, FOXM1, MCM7 and CDCA5) selected of YKT6 co-related genes, cell division cycle 20 (CDC20) promotes the resistance of glioblastoma (GBM) cells to chemotherapy and radiotherapy, while knockout of CDC20 can enhance the sensitivity of GBM cells to radiotherapy and chemotherapy by regulating the pro-apoptotic protein Bim [31].The polo-like kinase 1 (PLK1) is a serine/threonine protein kinase with a key role in eukaryotic cell division, DNA replication, and TP53 regulation [32]. PLK1 can promote the progress of Kras/TP53-mutated LUAD by regulating the transcriptional activation receptor RET [33]. In addition, PLK1 is overexpressed in hepatocellular carcinoma (HCC), related to tumor invasiveness and poor prognosis [34]. Cell division cycle-related genes 8 (CDCA8) and CDCA5 belong to the family of cell division cycle related genes. Studies have shown that miR-133a-3p can target CDCA8 and inhibit the progress of ESCA [35]. TPX2 can enhance the expression of cyclin-dependent kinase-1 (CDK1) in PRAD, then promote the phosphorylation of the ERK/GSK3b/Snail pathway, and finally EMT [36]. Kinesin family protein 2 C (KIF2C), also known as mitotic centromere-associated driving protein, encodes proteins in microtubule depolymerization, thus promoting chromosome separation during mitosis. KIF2C is highly expressed in HCC, related to tumor histological grade, pathological stage, and poor prognosis. In addition, KIF2C can promote the progression of HCC by activating the renin-angiotensin system (RAS)/mitogen-activated protein kinase (MAPK) and phosphatidylinositol 3-kinase (PI3K)/protein kinase B (PKB) signaling pathways [37]. Kinesin family member 23 (KIF23) is a member of the Kinesin family, highly expressed in triple-negative breast cancer (TNBC). Silencing of KIF23 expression can inhibit the proliferation and migration of the TNBC cells [38]. Recent research has demonstrated that KIF4A expression is up-regulated in LUAD and correlates with the prognosis of the patients [39]. Additionally, it has been reported that miR-877-5p could inhibit cell growth by directly targeting FOXM1, potentially furnishing a promising biomarker for targeted therapy in NSCLC [40]. MCM7 belongs to the small chromosome maintenance protein family, with a pivotal role in DNA replication and proliferation in eukaryotic cells. Several studies indicated that receptor for activated C kinase1 (RACK1) could modulate the growth and cell cycle progression of human NSCLC cells through MCM7 phosphorylation mediated by the MCM7/RACK1/Akt signal complex [41]. CDCA5 plays an important role in the occurrence and development of many kinds of cancers

by regulating cell cycle. CDCA5 is highly expressed in breast cancer tissues and cell lines. CDCA5 deletion can inhibit cell proliferation, invasion, and migration. Hence, CDCA5 can be used as a prognostic biomarker and therapeutic target for breast cancer [42]. Accordingly, the aforementioned hub genes associated with YKT6 are all correlated with tumor progression and prognosis, exhibiting functions that influence tumor cell proliferation, invasion, and migration.

Enrichment analysis of YKT6 and its associated genes revealed that the predominant physiological functions involved cell division, mitosis, and the cell cycle. Consistently, the majority of the hub genes identified were related to the cell cycle. GSEA demonstrated that YKT6 may exert its effects in LUAD through the PLK1 and TP53 pathways (Supplementary Table 4). Furthermore, as previously noted, PLK1 has been shown to facilitate the progression of LUAD with K-ras/TP53 mutations by modulating the transcriptional activation of the RET receptor. This suggests that there may be a significant interplay between YKT6 and PLK1 in the genesis and progression of LUAD, a relationship that warrants further investigation.

In recent years, tumor immune evasion has emerged as a central focus in anti-cancer therapies. The tumor microenvironment is composed of a multitude of immune cells, including macrophages, T cells, and NK cells, which can directly or indirectly influence the milieu surrounding tumor cells and modulate their biological activities. Consequently, immune cell therapy holds broad potential for the treatment of LUAD. YKT6 has been implicated in the infiltration of immune cells in LUAD, with increased immune cell infiltration being correlated with higher expression levels of YKT6, thus laying a foundational basis for effective immunotherapy. These findings offer innovative perspectives on the immunotherapeutic approach for LUAD patients.

In summary, our current study posits YKT6 as a potential novel biomarker for LUAD. Nevertheless, the precise mechanisms through which YKT6 regulates the onset and progression of LUAD remain elusive. Further research, accompanied by clinical validation, is essential to unravel the molecular underpinnings of YKT6 in both the genesis and therapeutic intervention of LUAD.

Conclusion

Collectively, this study provides a comprehensive demonstration of the upregulated expression of YKT6 in LUAD and its correlation with the adverse prognosis of LUAD patients. It holds promise as an innovative prognostic and diagnostic biomarker for LUAD.

Supplementary Information

The online version contains supplementary material available at https://doi.org/10.1186/s12885-024-12975-3.

Supplementary Material 1: Supplementary Fig. 1. GSEA of YKT6 DEGs in LUAD

Supplementary Material 2: Supplementary Fig. 2. The mRNA expression of the ten selected hub genes in LUAD based on TCGA database. (A) CDC20. (B) PLK1. (C) CDCA8. (D) TPX2. (E) KIF2C. (F) KIF23. (G) KIF4A. (H) FOXM1. (I) MCM7. (J) CDCA5

Supplementary Material 3: Supplementary Fig. 3. The prognosis of the ten selected hub genes in LUAD from Kaplan-Meier plotter. (A) CDC20. (B) PLK1. (C) CDCA8. (D) TPX2. (E) KIF2C. (F) KIF23. (G) KIF4A. (H) FOXM1. (I) MCM7. (J) CDCA5

Supplementary Material 4

Supplementary Material 5

Supplementary Material 6

Supplementary Material 7

Supplementary Material 8: Supplementary Fig. 4. Relationship between YKT6 expression and clinical features in UALCAN. Correlation of YKT6 mRNA expression with clinical stage (A), lymph node metastasis (B), smoking history (C) and TP53 mutation (D)

Acknowledgements

The authors gratefully acknowledge contributions from the TCGA network the authors listed in this manuscript.

Author contributions

Liming Zhang, Shaoqiang Wang and Lina Wang designed and performed bioinformatics analysis. Liming Zhang and Lina Wang analyzed the data and organized pictures. Liming Zhang, Lina Wang and Shaoqiang Wang wrote and revised the paper. All authors read and approved the final version of the manuscript.

Funding

This work was supported by the National Natural Science Foundation of China (81800182, 81802290). The funders had no role in study design, data collection and analysis, decision to publish, or preparation of the manuscript.

Data availability

Data availability Publicly available datasets were analyzed in this study. All data generated in the study are included in the present article and supplementary data.

Declarations

Ethics approval and consent to participate

This study was conducted in accordance with the ethical standards as outlined in the 1964 Declaration of Helsinki and its later amendments. Approval was obtained from the Ethics Committee of the Affiliated Hospital of Jining Medical University, with the reference number 2021-11-C009. And written informed consent was obtained before surgery from each patient.

Consent for publication

Not applicable.

Competing interests

The authors declare no competing interests.

Author details

[1]Medical Research Center, Affiliated Hospital of Jining Medical University, Jining Medical University, 89 Guhuai Road, Jining, Shandong 272029, P.R. China
[2]Department of Thoracic Surgery, Weifang Second People's Hospital, Weifang, Shandong 261041, P.R. China

[3]Department of Thoracic Surgery, Weifang People's Hospital, Weifang, Shandong 261000, P.R. China

Received: 12 July 2024 / Accepted: 23 September 2024
Published online: 07 October 2024

References

1. Bray F, Laversanne M, Sung H, Ferlay J, Siegel RL, Soerjomataram I, Jemal A. Global cancer statistics 2022: GLOBOCAN estimates of incidence and mortality worldwide for 36 cancers in 185 countries. CA Cancer J Clin. 2024;74:229–63.
2. Rodriguez-Canales J, Parra-Cuentas E. Wistuba, II, diagnosis and molecular classification of Lung Cancer. Cancer Treat Res. 2016;170:25–46.
3. Hasan N, Kumar R, Kavuru MS. Lung cancer screening beyond low-dose computed tomography: the role of novel biomarkers. Lung. 2014;192:639–48.
4. Kassem K, Shapiro M, Gorenstein L, Patel K, Laird C. Evaluation of high-risk pulmonary nodules and pathologic correlation in patients enrolled in a low-dose computed tomography (LDCT) program. J Thorac Dis. 2019;11:1165–9.
5. Molina JR, Yang P, Cassivi SD, Schild SE, Adjei AA. Non-small cell lung cancer: epidemiology, risk factors, treatment, and survivorship. Mayo Clin Proc. 2008;83:584–94.
6. Li X, Gu G, Soliman F, Sanders AJ, Wang X, Liu C. The Evaluation of Durative Transfusion of Endostar Combined with Chemotherapy in Patients with Advanced Non-Small Cell Lung Cancer, Chemotherapy, 63 (2018) 214–219.
7. Stella GM, Luisetti M, Pozzi E, Comoglio PM. Oncogenes in non-small-cell lung cancer: emerging connections and novel therapeutic dynamics. Lancet Respir Med. 2013;1:251–61.
8. Filippini F, Rossi V, Galli T, Budillon A, D'Urso M. D'Esposito, Longins: a new evolutionary conserved VAMP family sharing a novel SNARE domain. Trends Biochem Sci. 2001;26:407–9.
9. Tochio H, Tsui MM, Banfield DK, Zhang M. An autoinhibitory mechanism for nonsyntaxin SNARE proteins revealed by the structure of Ykt6p. Science. 2001;293:698–702.
10. Rikitake Y. Regulation of the SNARE protein Ykt6 function by diprenylation and phosphorylation. J Biochem. 2022;172:337–40.
11. McNew JA, Sogaard M, Lampen NM, Machida S, Ye RR, Lacomis L, Tempst P, Rothman JE, Söllner TH. Ykt6p, a prenylated SNARE essential for endoplasmic reticulum-golgi transport. J Biol Chem. 1997;272:17776–83.
12. Yang Z, Yan G, Zheng L, Gu W, Liu F, Chen W, Cui X, Wang Y, Yang Y, Chen X, Fu Y, Xu X. YKT6, as a potential predictor of prognosis and immunotherapy response for oral squamous cell carcinoma, is related to cell invasion, metastasis, and CD8 + T cell infiltration. Oncoimmunology. 2021;10:1938890.
13. Xu JZ, Jiang JJ, Xu HJ, Sun XD, Liu ZC, Hu ZM. High expression of YKT6 associated with progression and poor prognosis of hepatocellular carcinoma. Scand J Gastroenterol. 2021;56:1349–54.
14. Ooe A, Kato K, Noguchi S. Possible involvement of CCT5, RGS3, and YKT6 genes up-regulated in p53-mutated tumors in resistance to docetaxel in human breast cancers. Breast Cancer Res Treat. 2007;101:305–15.
15. Tomczak K, Czerwińska P, Wiznerowicz M. The Cancer Genome Atlas (TCGA): an immeasurable source of knowledge. Contemp Oncol (Pozn). 2015;19:A68–77.
16. Navani S. Manual evaluation of tissue microarrays in a high-throughput research project: the contribution of Indian surgical pathology to the human protein atlas (HPA) project. Proteomics. 2016;16:1266–70.
17. Győrffy B. Transcriptome-level discovery of survival-associated biomarkers and therapy targets in non-small-cell lung cancer. Br J Pharmacol. 2024;181:362–74.
18. Győrffy B. Integrated analysis of public datasets for the discovery and validation of survival-associated genes in solid tumors. Innov (Camb). 2024;5:100625.
19. Hänzelmann S, Castelo R, Guinney J. GSVA: gene set variation analysis for microarray and RNA-seq data. BMC Bioinformatics. 2013;14:7.
20. Li T, Fan J, Wang B, Traugh N, Chen Q, Liu JS, Li B, Liu XS. TIMER: a web server for Comprehensive Analysis of Tumor-infiltrating Immune cells. Cancer Res. 2017;77:e108–10.
21. Warde-Farley D, Donaldson SL, Comes O, Zuberi K, Badrawi R, Chao P, Franz M, Grouios C, Kazi F, Lopes CT, Maitland A, Mostafavi S, Montojo J, Shao Q, Wright G, Bader GD, Morris Q. The GeneMANIA prediction server: biological network integration for gene prioritization and predicting gene function. Nucleic Acids Res. 2010;38:W214–220.
22. Gao J, Aksoy BA, Dogrusoz U, Dresdner G, Gross B, Sumer SO, Sun Y, Jacobsen A, Sinha R, Larsson E, Cerami E, Sander C, Schultz N. Integrative analysis of complex cancer genomics and clinical profiles using the cBioPortal. Sci Signal. 2013;6:pl1.
23. Aran D, Camarda R, Odegaard J, Paik H, Oskotsky B, Krings G, Goga A, Sirota M, Butte AJ. Comprehensive analysis of normal adjacent to tumor transcriptomes. Nat Commun. 2017;8:1077.
24. Lopes CT, Franz M, Kazi F, Donaldson SL, Morris Q, Bader GD. Cytoscape web: an interactive web-based network browser. Bioinformatics. 2010;26:2347–8.
25. Huang da W, Sherman BT, Lempicki RA. Systematic and integrative analysis of large gene lists using DAVID bioinformatics resources. Nat Protoc. 2009;4:44–57.
26. Sherman BT, Hao M, Qiu J, Jiao X, Baseler MW, Lane HC, Imamichi T, Chang W. DAVID: a web server for functional enrichment analysis and functional annotation of gene lists (2021 update). Nucleic Acids Res. 2022;50:W216–21.
27. Yan Y, Xu Z, Qian L, Zeng S, Zhou Y, Chen X, Wei J, Gong Z. Identification of CAV1 and DCN as potential predictive biomarkers for lung adenocarcinoma. Am J Physiol Lung Cell Mol Physiol. 2019;316:L630–43.
28. DeSantis CE, Miller KD, Dale W, Mohile SG, Cohen HJ, Leach CR, Goding Sauer A, Jemal A, Siegel RL. Cancer statistics for adults aged 85 years and older, 2019. CA Cancer J Clin. 2019;69:452–67.
29. Zhang C, Leighl NB, Wu YL, Zhong WZ. Emerging therapies for non-small cell lung cancer. J Hematol Oncol. 2019;12:45.
30. Zhou M, Wang H, Zeng X, Yin P, Zhu J, Chen W, Li X, Wang L, Wang L, Liu Y, Liu J, Zhang M, Qi J, Yu S, Afshin A, Gakidou E, Glenn S, Krish VS, Miller-Petrie MK, Mountjoy-Venning WC, Mullany EC, Redford SB, Liu H, Naghavi M, Hay SI, Wang L, Murray CJL, Liang X. Mortality, morbidity, and risk factors in China and its provinces, 1990–2017: a systematic analysis for the global burden of Disease Study 2017. Volume 394. Lancet; 2019. pp. 1145–58.
31. Mao DD, Cleary RT, Gujar A, Mahlokozera T, Kim AH. CDC20 regulates sensitivity to chemotherapy and radiation in glioblastoma stem cells. PLoS ONE. 2022;17:e0270251.
32. Liu XS, Song B, Liu X. The substrates of Plk1, beyond the functions in mitosis. Protein Cell. 2010;1:999–1010.
33. Kong Y, Allison DB, Zhang Q, He D, Li Y, Mao F, Li C, Li Z, Zhang Y, Wang J, Wang C, Brainson CF, Liu X. The kinase PLK1 promotes the development of Kras/Tp53-mutant lung adenocarcinoma through transcriptional activation of the receptor RET. Sci Signal. 2022;15:eabj4009.
34. He ZL, Zheng H, Lin H, Miao XY, Zhong DW. Overexpression of polo-like kinase1 predicts a poor prognosis in hepatocellular carcinoma patients. World J Gastroenterol. 2009;15:4177–82.
35. Wang X, Zhu L, Lin X, Huang Y, Lin Z. MiR-133a-3p inhibits the malignant progression of oesophageal cancer by targeting CDCA8. J Biochem. 2022;170:689–98.
36. Zhang B, Zhang M, Li Q, Yang Y, Shang Z, Luo J. TPX2 mediates prostate cancer epithelial-mesenchymal transition through CDK1 regulated phosphorylation of ERK/GSK3β/SNAIL pathway. Biochem Biophys Res Commun. 2021;546:1–6.
37. Mo S, Fang D, Zhao S, Thai Hoa PT, Zhou C, Liang T, He Y, Yu T, Chen Y, Qin W, Han Q, Su H, Zhu G, Luo X, Peng T, Han C. Down regulated oncogene KIF2C inhibits growth, invasion, and metastasis of hepatocellular carcinoma through the Ras/MAPK signaling pathway and epithelial-to-mesenchymal transition. Ann Transl Med. 2022;10:151.
38. Jian W, Deng XC, Munankarmy A, Borkhuu O, Ji CL, Wang XH, Zheng WF, Yu YH, Zhou XQ, Fang L. KIF23 promotes triple negative breast cancer through activating epithelial-mesenchymal transition. Gland Surg. 2021;10:1941–50.
39. Song Y, Tang W, Li H. Identification of KIF4A and its effect on the progression of lung adenocarcinoma based on the bioinformatics analysis. Biosci Rep. 2021;41.
40. Liu Z, Wang X, Cao L, Yin X, Zhang Q, Wang L. MicroRNA-877-5p Inhibits Cell Progression by Targeting FOXM1 in Lung Cancer, Can Respir J, 2022 (2022) 4256172.
41. Fei L, Ma Y, Zhang M, Liu X, Luo Y, Wang C, Zhang H, Zhang W, Han Y. RACK1 promotes lung cancer cell growth via an MCM7/RACK1/ akt signaling complex. Oncotarget. 2017;8:40501–13.

42. Hu H, Xiang Y, Zhang XY, Deng Y, Wan FJ, Huang Y, Liao XH, Zhang TC. CDCA5 promotes the progression of breast cancer and serves as a potential prognostic biomarker. Oncol Rep. 2022;48.

Publisher's note